Ultra-Large-Pore Mesoporous Carbons Templated from Poly(ethylene oxide)-*b*-Polystyrene Diblock Copolymer by Adding Polystyrene Homopolymer as a Pore Expander

Yonghui Deng, Jia Liu, Chong Liu, Dong Gu, Zhenkun Sun, Jing Wei, Junyong Zhang, Lijuan Zhang, Bo Tu, and Dongyuan Zhao*

Department of Chemistry, Shanghai Key Laboratory of Molecular Catalysis and Innovative Materials, Key Laboratory of Molecular Engineering of Polymers of Ministry of Education and Advanced Materials Laboratory, Fudan University, Shanghai 200433, P. R. China

Received September 6, 2008. Revised Manuscript Received October 14, 2008

A pore swelling approach was developed for the synthesis of ultralarge mesoporous carbons by using diblock copolymer PEO_{125}-*b*-PS_{230} as a template, homopolystyrene (*h*-PS_{49}) as a pore expander, resol as a carbon source, and THF as a solvent through solvent evaporation induced self-assembly (EISA). Small-angle X-ray scattering (SAXS) and transmission electron microscopy (TEM) characterizations show that when *h*-PS_{94} amount is lower than 20 wt% relative to PEO_{125}-*b*-PS_{230}, highly ordered face-center cubic (fcc) mesoporous carbon structure (space group $Fm\bar{3}m$) with ultralarge cell parameter of 46.4−58.0 nm can be obtained. Nitrogen sorption measurements reveal that the obtained LP-FDU-18s possess high surface area of about 1210 m^2/g and large pore volume of 1.10 cm^3/g. Because of adding pore swelling agent *h*-PS_{49}, the mesostructural shrinkage is restrained, the pore wall thickness becomes very thin (3.6 nm). With the increase of *h*-PS_{49} addition amount from 0 to 20 wt%, the pore size can be continuously tuned in the range of 22.9−37.4 nm. Excess *h*-PS_{49} addition can lead to foamlike disordered porous carbons with multimodal pore size distribution (40−90 nm). A continuous solubilizing process is proposed to explain the expansion of pore size and cell parameter. This approach could be extended to the synthesis of other large-pore mesoporous materials with different frameworks such as silica, silica-carbon composite, and metal oxides.

Downloaded via HARVARD UNIV on July 11, 2019 at 12:44:38 (UTC).
See https://pubs.acs.org/sharingguidelines for options on how to legitimately share published articles.

Introduction

Since the synthesis of the ordered mesoporous carbon (OMC) was first reported in 1999[1] by using mesoporous silica as a hard template, it has gained considerable attention because of its potential applications in adsorption, catalysis, fuel cell, energy storage, and so on.[2−4] Using this hard templating approach, researchers have successfully synthesized a variety of OMC replicates with variable reversed mesostructures.[5−14] Recently, an organic−organic assembly approach has been developed for direct synthesis of ordered mesoporous carbons with continuous frameworks.[15−23] By using poly(ethylene oxide)-*b*-poly(propylene oxide)-*b*-poly(ethylene oxide) (PEO-PPO-PEO) triblock copolymers as templates and phenolic resol as a carbon source, researchers have successfully obtained a family of high-quality OMCs with diverse pore structures.[15−19] This innovative method escapes from the complicated hard templating procedures, and therefore represents a breakthrough in the synthesis of OMC materials. The key of the synthesis is the formation of highly ordered organic−organic nanocomposites consisting of thermosetting polymer resin precursors and thermally decomposable PEO-PPO-PEO templates driven by hydrogen-

* E-mail: dyzhao@fudan.edu.cn, Web: http://homepage.fudan.edu.cn/~dyzhao/default.htm. Tel: 86-21-5566-4194. Fax: 86-21-5566-4192.

(1) Ryoo, R.; Joo, S. H.; Jun, S. *J. Phys. Chem. B* **1999**, *103*, 7743.
(2) Kinoshita, K. In *Carbon: Electrochemical and Physicochemical Properties*; John Wiley & Sons: New York, 1987.
(3) Diddams, P. *Inorganic Supports and Catalysts*; Smith, K., Ed.; Ellis Horwood: New York, 1992; pp 3−39.
(4) Patrick, J. W. In *Porosity in Carbons: Characterization and Applications*; Edward Arnold: London, 1995.
(5) Gierszal, K. P.; Kim, T.-W.; Ryoo, R.; Jaroniec, M. *J. Phys. Chem. B* **2005**, *109*, 23263.
(6) Yang, H.; Yan, Y.; Liu, Y.; Zhang, F. Q.; Zhang, R. Y.; Meng, Y.; Li, M.; Xie, S. H.; Tu, B.; Zhao, D. Y. *J. Phys. Chem. B* **2004**, *108*, 17320.
(7) Jun, S.; Jo, S. H.; Ryoo, R.; Kruk, M.; Jaroniec, M.; Liu, Z.; Oshuna, T.; Terasaki, O. *J. Am. Chem. Soc.* **2000**, *122*, 10712.
(8) Lee, J.; Yoon, S.; Oh, S.; Shin, M.; Hyeon, T. *Adv. Mater.* **2000**, *12*, 359.
(9) Kim, S.; Pinnavaia, T. J. *Chem. Commun.* **2001**, 2418.
(10) Vinu, A. *Adv. Funct. Mater.* **2008**, *18*, 816.
(11) Lee, J.; Kim, J.; Hyeon, T. *Adv. Mater.* **2006**, *18*, 2073.
(12) Lu, A. H.; Schmidt, W.; Spliethoff, B.; Schuth, F. *Adv. Mater.* **2003**, *15*, 1602.
(13) Fan, J.; Yu, C. Z.; Wang, L. M.; Tu, B.; Zhao, D. Y.; Sakamoto, Y.; Terasaki, O. *J. Am. Chem. Soc.* **2001**, *123*, 12113.
(14) Lu, A.; Kiefer, A.; Schmidt, W.; Schüth, F. *Chem. Mater.* **2004**, *16*, 100.
(15) Meng, Y.; Gu, D.; Zhang, F. Q.; Shi, Y. F.; Yang, H.; Tu, B.; Yu, C. Z.; Zhao, D. Y. *Angew. Chem, Int. Ed.* **2005**, *44*, 7053.
(16) Meng, Y.; Gu, D.; Zhang, F. Q.; Shi, Y. F.; Cheng, L.; Feng, D.; Wu, Z. X.; Chen, Z. X.; Wan, Y.; Stein, A.; Zhao, D. Y. *Chem. Mater.* **2006**, *18*, 4447.
(17) Zhang, F. Q.; Meng, Y.; Gu, D.; Yan, Y.; Yu, C. Z.; Tu, B.; Zhao, D. Y. *J. Am. Chem. Soc.* **2005**, *127*, 13508.
(18) Liang, C.; Dai, S. *J. Am. Chem. Soc.* **2006**, *128*, 5316.
(19) Wan, Y.; Shi, Y. F.; Zhao, D. Y. *Chem. Mater.* **2008**, *20*, 932.
(20) Kim, T. W.; Solovyov, L. A. *J. Mater. Chem.* **2006**, *16*, 1445.
(21) Liu, R. L.; Shi, Y. F.; Wan, Y.; Meng, Y.; Zhang, F. Q.; Gu, D.; Chen, Z. X.; Tu, B.; Zhao, D. Y. *J. Am. Chem. Soc.* **2006**, *128*, 11652.
(22) Liang, C.; Hong, K.; Guiochon, G. A.; Mays, J. M.; Dai, S. *Angew. Chem., Int. Ed.* **2004**, *43*, 5785.
(23) Wang, J.; Matyjaszewski, K. *J. Am. Chem. Soc.* **1995**, *117*, 5614.

10.1021/cm802413q CCC: $40.75 © 2008 American Chemical Society
Published on Web 11/08/2008

bonding interaction through cooperative assembly or solvent evaporation induced self-assembly (EISA) process.

Large-pore OMCs are much desirable for applications involving large molecules, because they can offer a fast diffusion rate of the guest molecules. Unfortunately, from the hard-templating approach, the replicated OMCs usually have the pore size smaller than 5.0 nm because of the difficulty in tuning the pore wall thickness of mesoporous silica templates.[20] In the case of organic−organic self-assembly, because of the molecule composition limitation for PEO-PPO-PEO templates and the enormous shrinkage of the phenolic resin frameworks during pyrolysis, the obtained OMCs have rather small mesopores less than 4.0 nm.[15−19] By using a triconstituent coassembly strategy to introduce nanosized silicates into the polymer frameworks for reducing the shrinkage, the resultant mesopore sizes are still limited to about 6 nm.[21] Recently, by using polystyrene-*b*-poly(4-vinylpyridine) (PS-*b*-P4VP) as a template and resorcinol-formaldehyde resins as a carbon source, Dai and co-workers[22] synthesized ordered and well-oriented mesoporous carbon thin films with pore size up to 36 nm. The preparation procedure involves a complicated stepwise assembly process assisted with solvent annealing treatment using mixed vapor of benzene and dimethyl formamide. The ultralarge pore size stems from the large molecular weight of the template and the annealing treatment which could significantly swell the PS microdomain of the ordered nanocomposites. More recently, we have prepared two kinds of high-molecular-weight amphiphilic diblock copolymers poly(ethylene oxide)-*b*-polystyrene (PEO-*b*-PS) and poly-(ethylene oxide)-*b*-poly (methyl methacrylate) (PEO-*b*-PMMA) via a versatile atom transfer radical polymerization (ATRP) technology.[23] By using PEO_{125}-*b*-PS_{230}[24] and PEO_{125}-*b*-$PMMA_{144}$[25] as templates, we synthesized OMCs with a large pore size of ∼23 nm and thick pore wall (11.5−12.4 nm) via the EISA approach. Large mesopore sizes are indebted to the long hydrophobic length of the templates. All of these copolymer templates are laboratory-made, but it is difficult to vary the pore size by using individual copolymer templates. Although great success has been achieved in effectively tuning the pore size of mesoporous silicas in a wide range by the addition of small organic molecules such as trimethylbenzene (TMB) as a swelling agent,[26−29] no work has been done to rationally adjust the pore sizes of OMCs.

Herein, we report for the first time a pore swelling approach to synthesize ultra-large-pore OMCs (designated as LP-FDU-18) with face-center cubic mesostructure (fcc, space group of $Fm\bar{3}m$) by using diblock copolymer PEO_{125}-*b*-PS_{230} as a template and adding low-molecular-weight homopolystyrene (M_n of 5100 g/mol, *h*-PS_{49}) as a pore expander. The mesopore size is tunable in the range of 22.9−37.4 nm by changing the amount of *h*-PS_{49} through an EISA process. Small-angle X-ray scattering (SAXS) and transmission electron microscopy (TEM) characterizations show that, when the *h*-PS_{94} amount is lower than 20 wt% relative to PEO_{125}-*b*-PS_{230}, highly ordered cubic mesoporous carbons with ultralarge cell parameter of 46.4−58.0 nm can be obtained. Nitrogen sorption measurements reveal that the obtained LP-FDU-18s possess high surface area of about 1210 m^2/g and large pore volume of 1.10 cm^3/g. Excessive *h*-PS_{49} can lead to foamlike disordered porous carbons that have multimodal pore size distribution.

Experimental Section

(1) Chemicals. Monomethoxy poly(ethylene oxide) (monomethoxy-PEO5000), 2-bromoisobutyryl bromide and *N*,*N*,*N*′,*N*′,*N*″- pentamethyldiethylenetriamine (PMDETA) were purchased from Acros Corp. Tetrahydrofuran (THF), pyridine, styrene, ether, CuBr, petroleum ether (60−90 °C), tetraethyl orthosilicate (TEOS), phenol, formalin solution (37 wt %), NaOH, and HCl were purchased from Shanghai Chemical Corp. Styrene was purified by filtrating through Al_2O_3 column. All other chemicals were used as received. Deionized water was used for all experiments. The resol precursors with low-molecule-weight (M_w < 500) were prepared according to a procedure reported previously.[24]

(2) Synthesis of Ultra-Large-Pore Mesoporous Carbons. The PEO_{125}-*b*-PS_{230} (*Mn* = 297000 g/mol) with narrow molecular weigh distribution (PDI = 1.17) was prepared through ATRP method.[24] The homopolymer *h*-PS_{49} was also synthesized via ATRP technology by using ethyl 2-bromoisobutyrate as an initiator.[23,24] The obtained *h*-PS has mean molecular weight (M_n) of 5100 g/mol and monodisperse molecular weight distribution (PDI = 1.05) determined by ^1H NMR and gel permeation chromatography (GPC). The ultralarge pore mesoporous carbons with variable pores size were prepared via EISA method by adding *h*-PS_{49} as a pore swelling agent and using PEO_{125}-*b*-PS_{230} as a template and resol as a carbon source in THF solution with desired weight ratios, followed by thermosetting, pyrolysis and carbonization (Scheme 1). For a typical synthesis, 2.0 g of the resol precursor in THF solution (20 wt %, containing 0.25 g of phenol and 0.15 g of formaldehyde) was mixed with 0.50 g of *h*-PS_{49} in THF solution (2.5 wt %) and 5.0 g of PEO_{125}-*b*-PS_{230} in THF solution (2.5 wt %) with stirring to form a homogeneous solution. Transparent membranes were obtained by pouring the solution into Petri dishes to evaporate THF at room temperature for 12 h, followed by further heating in an oven at 100 °C for 24 h. The as-made product was scraped and crushed into powders. Pyrolysis was carried out in a tubular furnace under N_2 for 3 h at 450 °C for the decomposition of PEO_{125}-*b*-PS_{230} template and *h*-PS pore expander, then at 800 °C for another 3 h for the carbonization of frameworks. The heating rate was 1 °C/min below 450 °C, 2 °C/min in the range of 450−600 °C, and 5 °C/min above 600 °C.

(3) Characterization and Measurement Methods. Fourier-transform infrared (FTIR) spectra were collected on a Nicolet Fourier spectrophotometer using KBr pellets. TGA measurements were carried out on a Mettler Toledo TGA-SDTA851 analyzer (Switzerland) from 25 to 800 °C under N_2 with a heating rate of 5 °C/min. SAXS patterns were taken on a Nanostar U small-angle X-ray scattering system (Bruker, Germany) using Cu K_a radiation (40 kV, 35 mA). The *d*-spacing values were calculated by the formula $d = 2\pi/q$. The wall thickness was calculated from $W_T = \sqrt{2}a/2 - D$, where *a* represents the cell parameter and *D* is the

(24) Deng, Y. H.; Yu, T.; Wan, Y.; Shi, Y. F.; Meng, Y.; Gu, D.; Zhang, L. J.; Huang, Y.; Liu, C.; Wu, X. J.; Zhao, D. Y. *J. Am. Chem. Soc.* **2007**, *129*, 1690.
(25) Deng, Y. H.; Liu, C.; Gu, D.; Yu, T.; Tu, B.; Zhao, D. Y. *J. Mater. Chem.* **2008**, *18*, 91.
(26) Zhao, D.; Feng, J.; Huo, Q.; Melosh, N.; Fredrickson, G. H.; Chmelka, B. F.; Stucky, G. D. *Science* **1998**, *279*, 548.
(27) Fan, J.; Yu, C. Z.; Lei, J.; Zhang, Q.; Li, T.; Tu, B.; Zhou, W.; Zhao, D. Y. *J. Am. Chem. Soc.* **2005**, *127*, 10794.
(28) Boissiere, C.; Martines, M. A. U.; Tokumoto, M.; Larbot, A.; Prouzet, E. *Chem. Mater.* **2003**, *15*, 509.
(29) Kim, S. S.; Karkamkar, A.; Pinnavaia, T. J.; Kruk, M.; Jaroniec, M. *J. Phys. Chem. B* **2001**, *105*, 7663.

Scheme 1. Formation Process of Ultra-Large-Pore Mesoporous Carbons by Adding Homopolymer *h*-PS Pore Expander

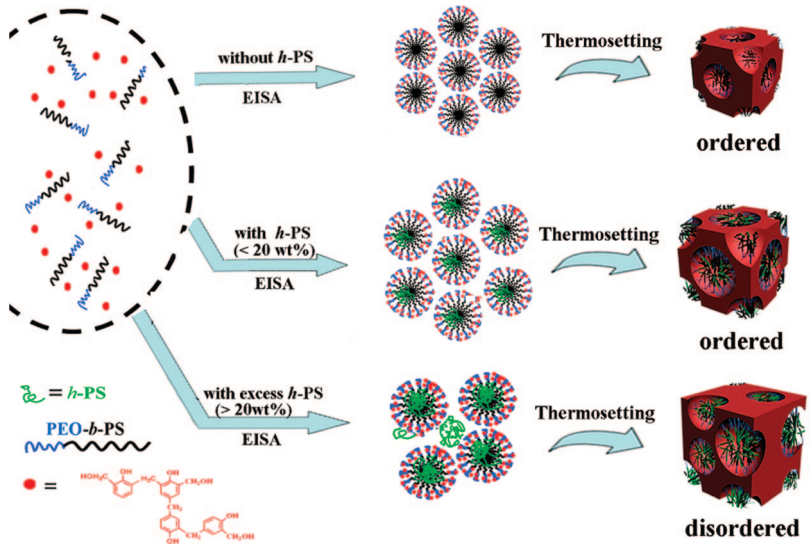

pore diameter calculated from the N_2 sorption. Nitrogen sorption isotherms were measured at 77 K with a Micromeritics Tristar 3000 analyzer. Before measurements, the samples were degassed in a vacuum at 200 °C for at least 6 h. The Brunauer−Emmett−Teller (BET) method was utilized to calculate the specific surface areas. By using the Broekoff-de Boer (BdB) sphere model, the pore volumes and pore size distributions were derived from the adsorption branches of isotherms, and the total pore volumes (V_t) were estimated from the adsorbed amount at a relative pressure P/P_0 of 0.992. TEM measurements were conducted on a JEOL 2011 microscope (Japan) operated at 200 kV. Raman spectra were obtained with a Dilor LabRam-1B microscopic Raman spectrometer (France), using a He−Ne laser with an excitation wavelength of 632.8 nm. The C, H, and O contents were measured on a Vario EL III elemental analyzer (Germany).

Results and Discussion

Because both the PEO-*b*-PS templates and *h*-Polystyrene are insoluble in water or ethanol, the EISA method in combination with pore swelling approach was employed to synthesize ultra large mesoporous carbons. After evaporation of the THF solvent, the LP-FDU-18 nanocomposites were undergone solidification at 100 °C and pyrolysis under N_2 at 450 °C for removal of the template and carbonization at 800 °C. The samples are denoted as LP-FDU-18-*X*-*Y*, where *X* and *Y* refer to the weight percent of *h*-PS_{49} relative to PEO_{125}-*b*-PS_{230} copolymer and the pyrolysis temperature, respectively. LP-FDU-18-2-450 sample prepared by using PEO_{125}-*b*-PS_{230} copolymer as a template and adding 2 wt % *h*-PS_{49} shows well-resolved SAXS patterns with five scattering peaks at *q*-values of 0.189, 0.365, 0.437, 0.651, and 0.901 nm^{-1}, respectively, which are similar to that for ordered mesoporous carbon sample LP-FDU-18-0-450 prepared without adding *h*-PS_{49} (Figure 1Aa, b). These peaks can be indexed to the 111, 311, 400, 440, and 644 (or 820) reflections of face-center cubic (fcc) mesostructure with the space group of $Fm\bar{3}m$, suggesting a highly ordered mesostructure. The cell parameter is calculated to be as large as 57.4 nm, which is much larger than that (52.8 nm) for the sample LP-FDU-18-0-450 without adding *h*-PS_{49} (Figure 1Aa, Table 1), clearly suggesting a swollen mesostructure. Further increasing the amount of *h*-PS_{49} (to 10 wt %), well-resolved SAXS patterns can also be observed (Figure 1Ac, d), indicating that the ordered fcc mesostructures are well-preserved. The cell parameter further increases to 61.1 nm, reflecting a continuous structure expansion. However, the SAXS pattern of LP-FDU-18-20-450 sample obtained with adding 20 wt % *h*-PS_{49} displays three resolved scattering peaks (Figure 1Ae), implying that the fcc mesostructure becomes a little degenerate. It could be attributed to the formation of distorted domains or defects in the mesostructure. Ultralarge cell parameters (~61.6 nm) can be obtained from the SAXS data. When the amount of *h*-PS_{49} further increases to as high as 25−35%, SAXS patterns show that the mesostructural regularity significantly decreases (see the Supporting Information, Figure S1), suggesting a disordered mesostructure. The *d*-spacings of first strong scatterings are calculated to be 38.3 and 42.2 nm, respectively, both larger than those of the ordered mesostructures with less *h*-PS addition.

After carbonization at 800 °C in N_2, all of LP-FDU-18-X-800 samples prepared by adding pore expander *h*-PS_{49} in the range of 0−20 wt % show similar well-resolved SAXS patterns (Figure 1B), indicating that the fcc ordered mesostructures are thermally stable. A large shift in the scattering peaks toward higher *q* values is observed, suggesting a mesostructural shrinkage (5.8−8.2%). The sample (LP-FDU-

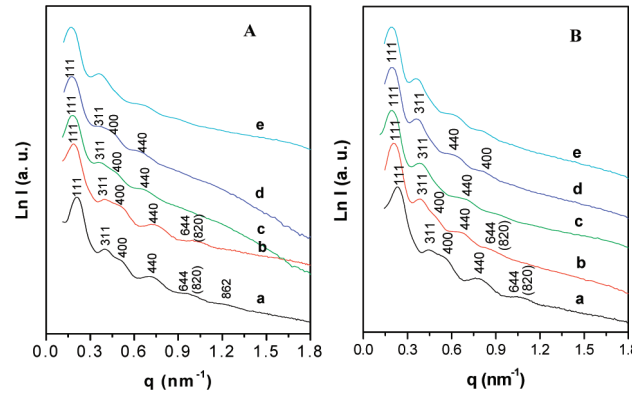

Figure 1. SAXS patterns of (A) LP-FDU-18-450 and (B) LP-FDU-18-800 samples with different *h*-PS/PEO_{125}-*b*-PS_{230} weight percents: (a) 0, (b) 2, (c) 5, (d) 10, and (e) 20%.

Table 1. Textural Properties of the Ultra-Large-Pore Ordered Mesoporous Carbon (LP-FDU-18) Materials Prepared by Using PEO_{125}-*b*-PS_{230} As a Template and Adding *h*-PS_{49} as a Pore Expander[a]

sample	d_{111} (nm)[b]	*a* (nm)[c]	structural shrinkage (%)	pore size (nm)	wall thickness (nm)[d]	BET surface area (m^2/g)	pore volume (cm^3/g)	micropore volume (cm^3/g)
FDU-18-0-450	30.5	52.8	12.1	26.0	11.3	353	0.45 (0.71)	0.16
(800)	(26.7)	(46.4)		(22.9)	(9.9)	(770)		(0.29)
FDU-18-2-450	33.1	57.4	6.4	30.5	10.0	366	0.52 (0.76)	0.19
(800)	(31.0)	(53.7)		(28.0)	(9.8)	(812)		(0.35)
FDU-18-5-450	34.5	59.7	8.2	35.4	6.8	394	0.61 (0.84)	0.22
(800)	(31.6)	(54.8)		(33.1)	(5.6)	(867)		(0.41)
FDU-18-10-450	35.3	61.1	5.9	39.1	4.1	423	0.73 (0.97)	0.27
(800)	(33.2)	(57.5)		(36.9)	(3.7)	(915)		(0.49)
FDU-18-20-450	35.6	61.6	5.8	39.4	4.2	490	0.87 (1.10)	0.31
(800)	(33.5)	(58.0)		(37.4)	(3.6)	(1210)		(0.52)
FDU-18-25-450	38.3							
(800)				(40−60)	(12[e])	(736)	(0.68)	(0.25)
FDU-18-35-450	42.2					(678)		
(800)				(40−90)	(15[e])		(0.72)	(0.28)

[a] The values in the brackets are data for the FDU-18-X-800 samples after carbonization at 800 °C. [b] The *d*-spacing values of 111 planes were calculated by the formula $d = 2\pi/q$. [c] The unit cell parameters (*a*) were calculated from the formula $a = d_{111}\sqrt{3}$. [d] The wall thickness values were calculated from $W_T = \sqrt{2}a/2 - D$, where *a* represents the cell parameter and *D* is the pore diameter. [e] Determined from TEM images.

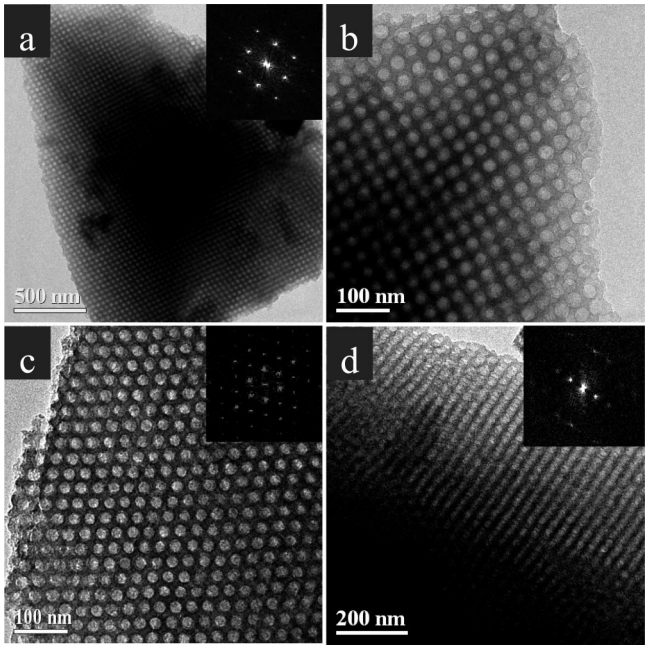

Figure 2. TEM images of mesoporous carbon LP-FDU-18-2-800 sample prepared by adding 2 wt % *h*-PS_{49} after carbonization at 800 °C viewed from (a, b) 100, (c) 110, and (d) 211 directions. The insets show the corresponding FFT diffractometers.

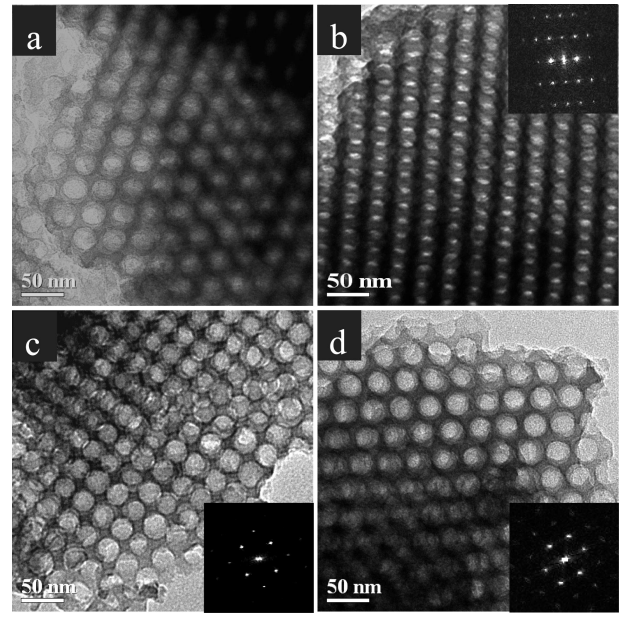

Figure 3. TEM images of LP-FDU-18-10-800 sample viewed from (a) 110 and (b) 211 directions, and FDU-18-20-800 sample viewed from (c) 100 and (d) 110 directions. The insets show the corresponding FFT diffractometers.

18-0-800) without *h*-PS exhibits much larger structure shrinkage (∼12.1%) than that with adding *h*-PS (<20 wt %) (Table 1). It implies that adding *h*-PS_{49} molecules can somehow retard the intense shrinkage during the carbonization.

The representative TEM images taken from the [100], [110] and [211] directions with corresponding Fourier diffractograms further confirm that LP-FDU-18-2-800 sample prepared by adding 2 wt % *h*-PS_{49} as the pore expander after carbonization at 800 °C has highly ordered cubic ($Fm\bar{3}m$) mesostructure (Figure 2). The cell parameter estimated from the TEM images is about 53 nm, consistent with the value from SAXS data (Table 1). Similarly, TEM images of LP-FDU-18-10-800 and LP-FDU-18-20-800 with larger amount of *h*-PS_{49} also show a high degree of periodicity over large domains viewed along [100], [110], and [211] directions, respectively. Furthermore, large sphere morphology can be obviously observed, confirming a highly ordered fcc mesostructure with large spherical pore cages (Figure 3). The unit cells estimated from these TEM images increase with the amount of *h*-PS_{49} and are larger than that of LP-FDU-18-0-800 without addition of *h*-PS_{49}, although the latter also shows high degree of periodicity over large-scale domains as revealed by TEM images (see the Supporting Information, Figure S2). It is worth noting that some domains with defects can be clearly observed in the TEM images of LP-FDU-18-20-800 sample (see the Supporting Information, Figure S3). It implies that large amount of *h*-PS_{49} can lead to distorted domains and even causes the mesostructure to degenerate. With excessive *h*-PS_{49} (25 and 35 wt %), TEM images show polydispersed size mesopores with disordered structure (Figure 4). The pore size of the LP-FDU-18-25-800 sample is roughly estimated in the ranges from 40 to 60 nm, whereas that for FDU-18-35-800 sample is in a wider range of 40−90 nm. It suggests that the excessive *h*-PS can lead to disordered foamlike carbon structures.

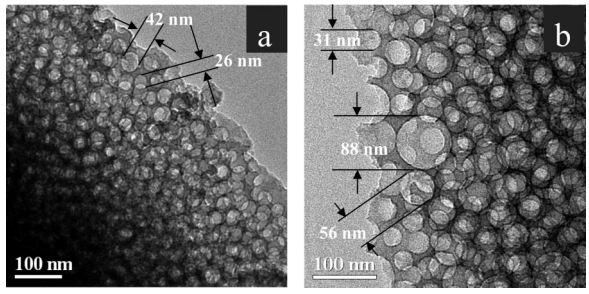

Figure 4. TEM images of (a) LP-FDU-18-25-800 and (b) LP-FDU-18-30-800 prepared by adding excessive *h*-PS_{49} (25 and 30 wt%) after carbonization at 800 °C under N_2.

All nitrogen isotherms of LP-FDU-18-X-450 samples prepared by adding *h*-PS_{49} as a pore expander (0−20 wt %) possess typical type IV curves with sharp capillary condensation steps in the relative pressure range of 0.86−0.97 (see the Supporting Information, Figure S4A), suggesting a uniform mesopore. Notably, the relative pressure for the capillary condensation increases with *h*-PS_{49} amount, indicating an increase of the mesopore size. Additionally, a very large H2-type hysteresis loop is observed, suggesting large caged mesopores with a small window size (<5.0 nm). Pore cavitation may form for the caged mesoporous materials during the desorption, because the size of the window approaches the critical value for the formation of cavitation (about 4 nm for nitrogen at 77 K).[30] The pore size distributions derived from adsorption branches using BdB sphere model show that all of the LP-FDU-18-*X*-450 samples are centered at the mean values of 26.0 ∼ 39.4 nm, increasing with *h*-PS_{49} addition amount (see the Supporting Information, Figure S4B). The pore wall thickness is calculated in the range of 11.3−4.2 nm (Table 1), dramatically decreasing with the increase of *h*-PS amount. It suggests that the addition of *h*-PS contributes more to the increase of the pore size than the increase in cell parameter. The LP-FDU-18-*X*-450 products have low BET surface areas around 350 − 490 m^2/g, increasing upon the *h*-PS_{49} amount (Table 1). Simultaneously, as the addition amount of *h*-PS_{49} increases, the total pore volume and micropore volume increase gradually from 0.45 to 0.87 cm^3/g and 0.16 to 0.31 cm^3/g, respectively (Table 1).

Similar to LP-FDU-18-*X*-400 samples, all of the LP-FDU-18-*X*-800 samples carbonized at 800 °C display representative type IV isotherms with sharp capillary condensation and large H_2-type hysteresis loops (Figure 5A), indicative of cagelike spherical mesopores with small entrance size. The pore size distributions show that the uniform mesopores are as large as 22.9−37.4 nm (Figure 5B). The dramatic decrease in the pore wall thickness with adding amount of *h*-PS_{49} is also observed (Table 1). The BET surface area of the samples is in the range of 770−1210 m^2/g, which is about twice higher than that of the LP-FDU-18-*X*-450 samples. Furthermore, the total pore volume and micropore volume increase with adding amount of *h*-PS_{49} up to 0.29 and 1.10 cm^3/g, respectively, which are significantly higher than those for the LP-FDU-18-*X*-450 samples, suggesting that a larger amount of micropores are generated during the carbonization at 800 °C.

When the amount of *h*-PS_{49} increases to 25−35 wt %, the resultant samples (LP-FDU-25-800 and LP-FDU-18-35-800) show broad capillary condensation steps at high relative pressure (P/P_0 = 0.91−0.98), suggesting a wide pore size distribution. Similarly, a huge hysteresis loop can be observed, indicating a small window size (see the Supporting Information, Figure S5A). It is worthy to note that the pore size distributions show bimodal and trimodal pores at mean values of 41.3, 59.2 nm, and 40.9, 63.8, 94.1 nm (see the Supporting Information, Figure S5B), suggesting disordered mesopore structures. Such multimodal pore size feature agrees well with the observations in the TEM images, which show pores of about 40 and 60 nm for LP-FDU-18-25-800 and about 40, 60, and 91 nm for LP-FDU-18-35-800, respectively (Figure 4).

Thermogravimetric analyses (TGA) show a weight loss of about 15 wt % below 210 °C due to the removal of physically adsorbed water in the porous channels[24] (see the Supporting Information, Figure S6). Large weight losses of 54 and 65 wt % at 300−800 °C are observed for the as-made LP-FDU-18-0 without *h*-PS and as-made LP-FDU-18-20 with 20 wt % *h*-PS, respectively, which can be ascribed to the decomposition of PEO_{125}-*b*-PS_{230} and *h*-PS_{49}, and pyrolysis of PF frameworks, suggesting that both template and pore expander can be removed at 450 °C. After carbonization at 800 °C, the yields for LP-FDU-18-0 and LP-FDU-18-20 are calculated to be 19 and 31 wt % based on carbon content, respectively, both much less than that (50 wt %) of PF, suggesting that the porosity makes for the decomposition and combustion. Elemental analysis of the LP-FDU-18-20-800 reveals that the framework is composed of C (90.3 wt %), H (2.9 wt %), and O (6.8 wt %) with C:H:O of 21.8:6.9:1 in molar ratio. The C content is comparable to that (∼92%) of mesoporous carbon reported previously,[16,17] suggesting that the carbonaceous frameworks are produced after pyrolysis at 800 °C. The Raman spectrum of LP-FDU-18-20-800 shows G band at 1595 cm^{-1} and D band at 1327 cm^{-1} (see the Supporting Information, Figure S7), implying a low degree of graphitization. The FT-IR spectrum of LP-FDU-18-20-800 further reveals a carbon framework feature after carbonization at 800 °C in N_2 (see the Supporting Information, Figure S8).

The ultralarge pore size of the ordered mesoporous carbon materials are attributed to the pore swelling effect exerted by the low molecular weight homopolymer *h*-PS_{49}. We proposed a continuous solubilizing process for swelling pore size and mesostructure in our study (Scheme 1). The PEO-*b*-PS copolymers can interact with resol precursors by hydrogen-bonding interaction and self-assemble to form ordered mesostructure during the solvent evaporation (Scheme 1a).[24] Because the chain length of homopolymer *h*-PS_{49} (∼5100 g/mol) is much shorter than that of the PS segment (∼15 000 g/mol) of PEO_{125}-*b*-PS_{230}, the affinity between *h*-PS_{49} and the hydrophobic PS segment with the same chain

(30) Ravikovitch, P. I.; Neimark, A. V. *Langmuir* **2002**, *18*, 9830.

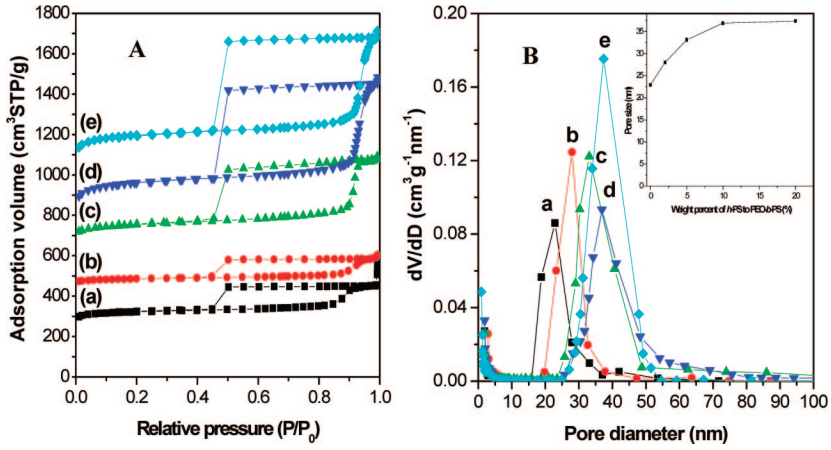

Figure 5. (A) N_2 isotherms and (B) pore size distribution of (a) LP-FDU-18-0-800, (b) LP-FDU-18-2-800, (c) LP-FDU-18-5-800, (d) LP-FDU-18-10-800 and (e) LP-FDU-18-20-800. The N_2 isotherms of b−e are offset vertically by 100, 300, 500, and 700 cm^3/g, respectively. The inset in part B shows the pore size changes of the LP-FDU-18-450 samples upon the increase of *h*-PS addition.

composition is much strong.[31] Therefore, a small amount of *h*-PS_{49} can continuously solubilize at the core of the PS microdomains of the diblock copolymer and swell the hydrophobic core volume. Such phenomena are quite general in diblock copolymer A-B segregation systems[32] driven by reducing the interaction enthalpy. In our case, during EISA process, PS-*b*-PEO diblock copolymer accommodates with a little amount of *h*-PS_{49} to form larger size sphere micelles and assemble with resol precursors to form the ordered mesostructured composites.[31] Therefore, *h*-PS_{49} homopolymer serves as an expander, and upon the increase of *h*-PS_{49} addition, the pore size and cell parameter can continuously increase without destroying the mesostructures (Scheme 1b). However, as predicted theoretically, [33,34] excessive *h*-PS can not be homogeneously accommodated in the PS microdomain, the microphase and macrophase separation simultaneously occur. As a result, only partial PS microdomains can be filled with more *h*-PS, and the wormlike disordered mesostructure with bimodal or even trimodal pore size distribution is formed (Scheme 1c). The strong affinity between the PS polymers can also draw back the PEO chain of PS-*b*-PEO templates, therefore, resulting in a thin wall thickness.

Conclusion

In summary, we have demonstrated a pore swelling approach for the synthesis of ultralarge mesoporous carbons by using diblock copolymer PEO_{125}-*b*-PS_{230} as a template, *h*-PS_{49} as a pore expander, resol as a carbon source and THF as a solvent through EISA. The products show highly ordered face-center cubic ($Fm\bar{3}m$) mesostructure with ultralarge pore size (up to 37.4 nm) and cell parameter (up to 58.0 nm), high surface area of about 1210 m^2/g and large pore volume of about 1.10 cm^3/g. Because of adding pore swelling agent *h*-PS_{49}, the mesostructural shrinkage is restrained, the pore wall thickness becomes very thin (3.6 nm). With the increase of *h*-PS_{49} addition amount from 0 to 20 wt %, BET surface area and pore volume increase, and pore size and cell parameter are continuously tunable in the range of 22.9−37.4 nm and 46.4−58.0 nm, respectively. Excess *h*-PS_{49} addition can lead to foamlike disordered porous carbons with multimodal pore size distribution (40−90 nm). A continuous solubilizing process is proposed for the expansion of pore size and cell parameter. Because of their high surface area, large pore size, and large pore volume, the obtained large-pore mesoporous carbons would have potential applications in chemical sensors, bioseparations, and fuel cells. This approach could be extended to synthesis of other large-pore mesoporous materials with different frameworks, such as silica, silica−carbon composite, and metal oxides.

Acknowledgment. This work was supported by the NSF of China (20721063, 20521140450, and 20871030), the State Key Basic Research Program of the PRC (2006CB202502 and 2006CB932302), Shanghai Nanotech Promotion Center (0652nm024), the Shanghai Science & Technology Committee (06DJ14006), Shanghai Leading Academic Discipline Project (B108), and the Shanghai Rising-Star Program (08QA14010). D.G. aknowledges financial support from the graduate student innovative research funds.

Note Added after ASAP Publication. The Acknowledgment section was revised from the version published ASAP November 8, 2008; the corrected version published ASAP November 13, 2008.

Supporting Information Available: SAXS patterns of LP-FDU-18-25-450 and LP-FDU-18-35-450; TEM images of LP-FDU-18-0-800 and FDU-18-20-800; N_2 isotherms and pore size distribution of LP-FDU-18-*x*-450, LP-FDU-18-25-800, and LP-FDU-18-35-800; TGA and DTG curves; Raman spectrum; and FT-IR spectra (PDF). This material is available free of charge via the Internet at http://pubs.acs.org.

CM802413Q

(31) Semenov, A. N. *Macromolecules* **1993**, *26*, 2273.
(32) Matsen, M. W. *Macromolecules* **1995**, *28*, 5765.
(33) Janert, P. K.; Schick, M. *Macromolecules* **1998**, *31*, 1109.
(34) Ceglie, K.; Fontell, A.; Lindman, B.; Ninham, B. *Acta Chem. Scand., A* **1986**, *40*, 247.